Angewandte Chemie
Eine Zeitschrift der Gesellschaft Deutscher Chemiker

Supporting Information

Single-Walled Carbon Nanotubes Encapsulated within Metallacycles

A. López-Moreno, S. Ibáñez, S. Moreno-Da Silva, L. Ruiz-González, N. M. Sabanés, E. Peris, E. M. Pérez**

SUPPORTING INFORMATION

Equipment

Thermogravimetric Analyses - TGA Thermogravimetric analyses were performed using a TA Instruments TGAQ500 with a ramp of 10 °C/min under air and nitrogen conditions from 100 to 1000 °C.

Raman spectroscopy - Raman spectra were recorded with a Bruker Senterra confocal Raman microscope (Bruker Optic, Ettlingen, Germany, resolution 9-15 cm^{-1}).

Ultraviolet/Visible/Near Infrared Spectroscopy – UV/VIS/NIR Spectroscopy UV-vis-NIR spectra were performed using a Cary 5000 UV/Vis/NIR spectrophotometer (Varian) and 10x10 mm quartz cuvettes (path length = 1 cm).

Atomic Force Microscopy - AFM AFM images were acquired using a JPK NanoWizard II AFM working in dynamic mode coupled to an inverted optical microscope Nikon Eclipse Ti-U. NT-MDT NSG01 silicon cantilevers, with typical values of 5.1 $N \cdot m^{-1}$ spring constant and 150 kHz resonant frequency, were employed under ambient conditions in air. The samples were dispersed in tetrachloroethane and spin coated onto mica slides.

Transmission Electron Microscopy - TEM Transmission electron microscopy (TEM) images were obtained in a JEOL-JEM 2100F (2.5 Å resolution) instrument operating at 200 kV. High resolution-transmission electron microscopy (HR-TEM) images were obtained in an imaging aberration corrected microscope JEOL JEM GRAND ARM300cF operating at 60 kV. Images were recorded on a slow-CCD camera GATAN Oneview. Approximately 0.2 mg of MINT was ultrasonic dispersed in 2 mL of tetrachloroethane for ten minutes. Few drops of this dispersion were deposited onto a 200 square mesh grid covered by holey carbon. After solvent evaporation in air, the grid was ready to use.

Synthesis of 1 and 2

Metallosquares **1**[1] and **2**[2] were synthesized as described in the literature.

Procedure for SWNTs Functionalization

MINT-1 (Route A)

(6,5)-SWNTs (5 mg) were dispersed in 5 mL of anhydrous acetonitrile by sonication in a bathsonicator. Then the pyrene-bis(imidazolium) salt (0.006 mmol, 2 eq), $[Pd(allyl)Cl]_2$ (0.003 mmol, 1 eq), $AgBF_4$ (0.006 mmol, 2 eq) and Cs_2CO_3 (0.012 mmol, 4 eq) were added. After 16 h at 60 ºC, MINT-**1** was recovered by filtration through a polytetrafluoroethylene (PTFE) membrane with a pore size of 0.2 μm and washed with CH_3CN and CH_2Cl_2 to remove all non-interlocked materials. The samples were dried under vacuum and subjected to thermogravimetric analysis (TGA) to quantify the degree of functionalization.

MINT-1 (Route B)

(6,5)-SWNTs (5 mg) were dispersed in 5 mL of TCE by sonication in a bathsonicator. Preformed metallosquare -**1** (0.0014 mmol) dissolved in 20 mL of TCE and 3 mL of CH_3CN was added. After 48 h at r.t. under dark, nanotubes were recovered by filtration through a polytetrafluoroethylene (PTFE) membrane with a pore size of 0.2 μm and washed with CH3CN and CH2Cl2 to remove all non-interlocked materials. The samples were dried under vacuum and subjected to thermogravimetric analysis (TGA) to quantify the degree of functionalization.

Metallosquare 2 + 6,5-SWCNTs

(6,5)-SWNTs (5 mg) were dispersed in 5 mL of TCE by sonication in a bath sonicator. Then bis-nickel-pyrene-di-imidazolylidene complex (5 mg, 1 eq), 4,4'-bipyridine (0.66 mg, 1 eq) and $AgBF_4$ (1.8 mg, 2 eq) were added. After 16 h at r.t , nanotubes were recovered by filtration through a polytetrafluoroethylene (PTFE) membrane with a pore size of 0.2 μm and washed with and CH_2Cl_2 and THF to remove all non-interlocked materials. The samples were dried under vacuum and subjected to thermogravimetric analysis (TGA) to quantify the degree of functionalization.

Reaction was also carried out in dry CH_2Cl_2 using same conditions.

Control experiments

(6,5)-SWNTs (5 mg) were dispersed in 5 mL of anhydrous acetonitrile by sonication in a bathsonicator. Then the pyrene-bis(imidazolium) salt (0.006 mmol, 2 eq), $[Pd(allyl)Cl]_2$ (0.003 mmol, 1 eq), and $AgBF_4$ (0.006 mmol, 2 eq) were added. After 16 h at 60 ºC, nanotubes were recovered by filtration through a polytetrafluoroethylene (PTFE) membrane with a pore size of 0.2 μm and washed with CH_3CN and CH_2Cl_2 to remove all non-interlocked materials. The samples were dried under vacuum and subjected to thermogravimetric analysis (TGA) to quantify the degree of functionalization.

(6,5)-SWNTs (5 mg) were dispersed in 5 mL of anhydrous acetonitrile by sonication in a bathsonicator. Then the pyrene-bis(imidazolium) salt (0.006 mmol, 2 eq), $AgBF_4$ (0.006 mmol, 2 eq) and Cs_2CO_3 (0.012 mmol, 4 eq) were added. After 16 h at 60 ºC, nanotubes were recovered by filtration through a polytetrafluoroethylene (PTFE) membrane with a pore size of 0.2 μm and washed with CH_3CN and CH_2Cl_2 to remove all non-interlocked materials. The samples were dried under vacuum and subjected to thermogravimetric analysis (TGA) to quantify the degree of functionalization.

(6,5)-SWNTs (10 mg) were dispersed in 10 mL of anhydrous acetonitrile by sonication in a bathsonicator and preformed metallo-square-1 (0.0014 mmol) was added. After 16 h at 60 ºC, nanotubes were recovered by filtration through a polytetrafluoroethylene (PTFE) membrane with a pore size of 0.2 μm and washed with CH_3CN and CH_2Cl_2 to remove all non-interlocked materials. The samples were dried under vacuum and subjected to thermogravimetric analysis (TGA) to quantify the degree of functionalization.

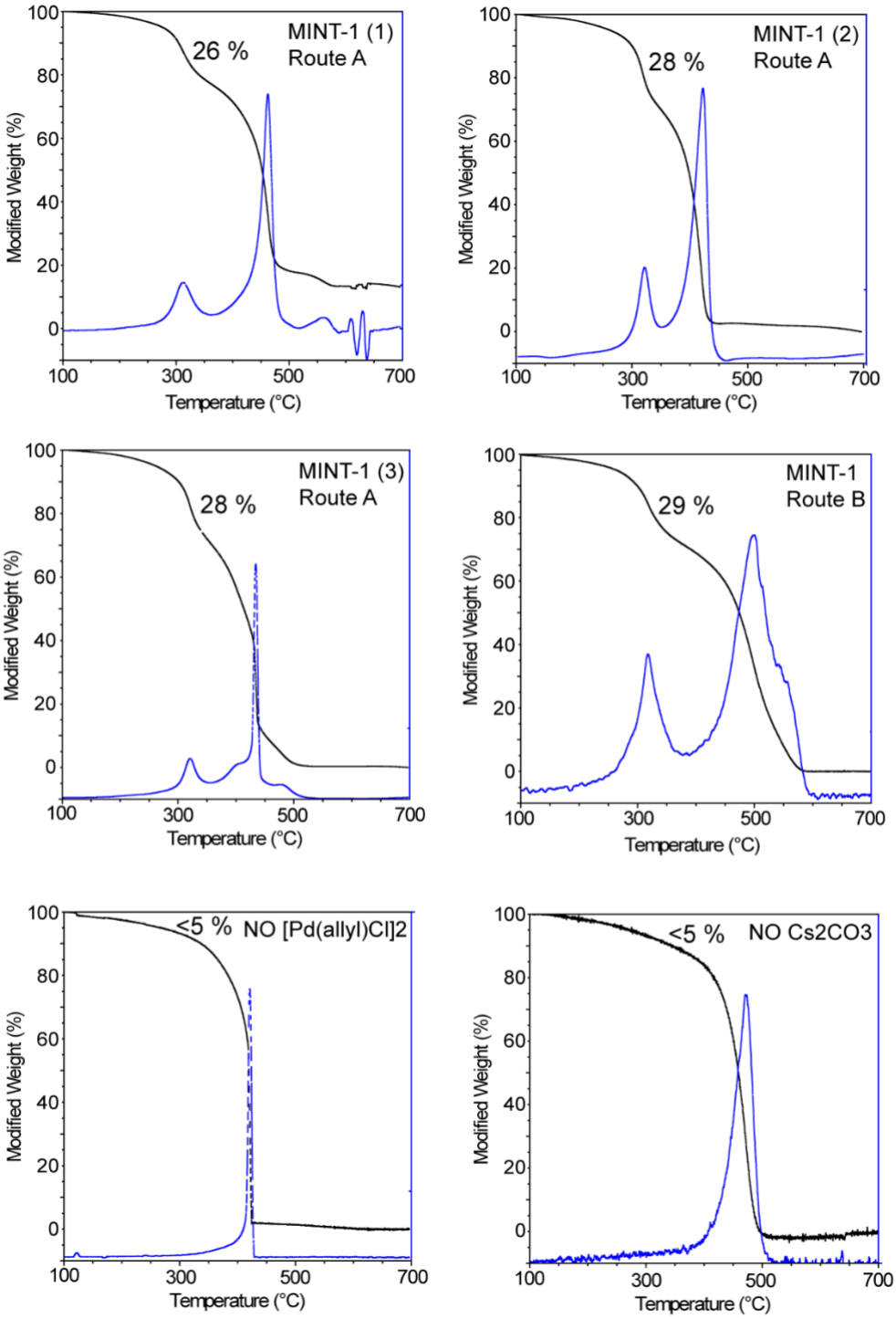

Figure S1. TGA analysis (under air, 10 ºC / min) of MINT-**1** (self-assembly), MINT-**1** (preformed metallosquare), and control experiments.

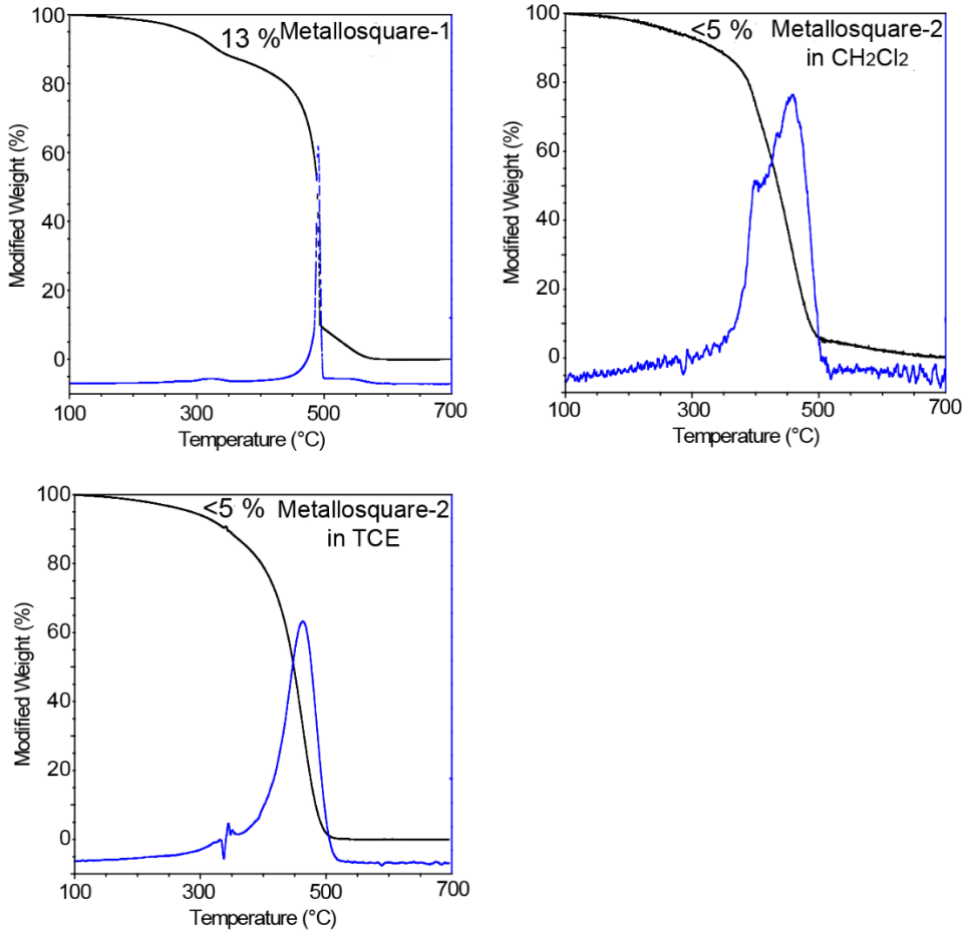

Figure S2. TGA analysis (under air, 10 ºC / min) of control experiment with preformed Metallosquare-**1** and Metallosquare-**2**.

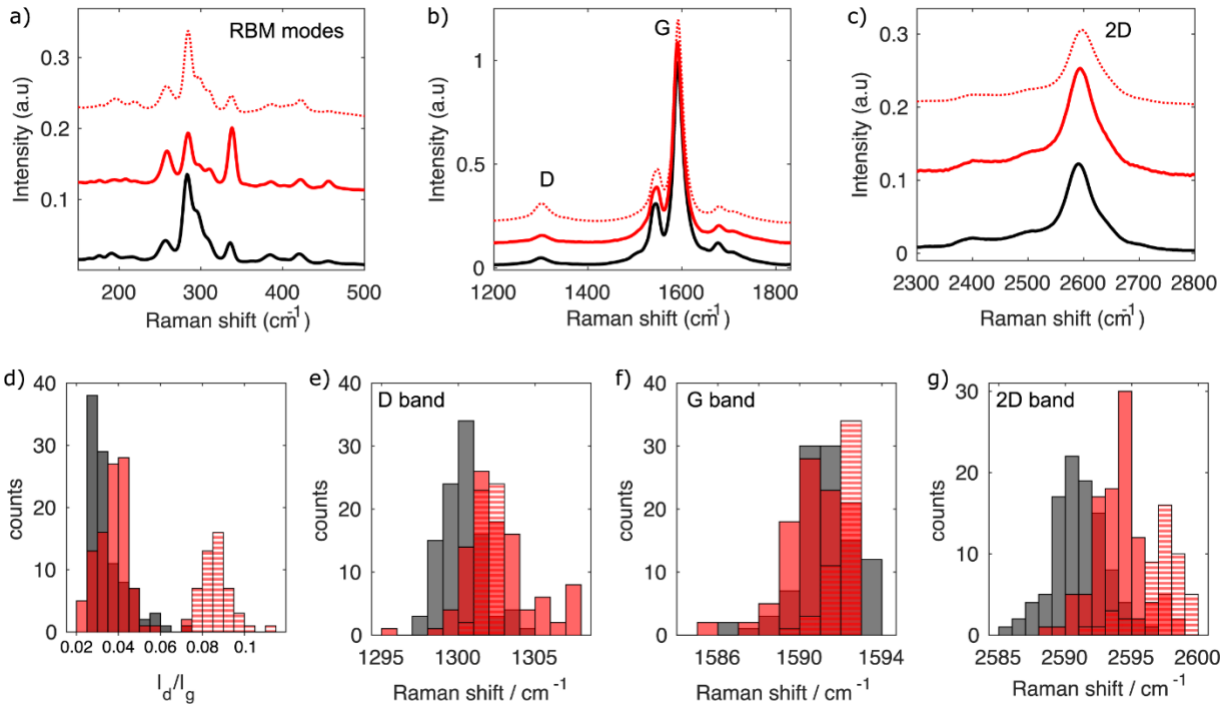

Figure S3 (a)-(c) Zoom into specific regions of the Raman spectra shown in Fig 2b in main text, showing a detail of the RBM (radial breathing modes), D and G (defect-induced and in-plane stretching, respectively) and 2D (overtone of D mode, also denoted G' by some authors) for (6,5)-SWCNT (black), MINT-**1** (self-assembly, red), and MINT-**1** (preformed metallosquare, dotted red). The displayed spectra are an average of 100 individual spectra acquired at different sample spots, statistical analysis of the spectral features of the individual spectra are displayed in: (d) intensity ratio (I_D/I_G); (e) D band position; (f) G^+ band position; (g) 2D band position for (6,5)-SWCNT (gray), MINT-**1** (self-assembly, solid red), and MINT-**1** (preformed metallosquare, dashed red). Spectra are acquired with 633 nm excitation light, 100x objective, 2 mW incident power, 5 sec acquisition time.

Raman spectra of the (6,5)-SWCNT (black) compared to the MINT-**1** (by self-assembly, red) and MINT-**1** (by encapsulation with preformed metallosquare, dotted red) are included in figure 2b of the main text. Zoom into specific spectral regions are included in Figure S3a to c. Figures S3 d) to g) contain histograms of intensity ratio (I_d/I_g), D, G and 2D band position of the individual spectra used for the averages ((6,5)-SWCNT gray, MINT-**1** (self-assembly, solid red) and MINT-**1**(preformed metallosquare, dashed red). The histograms are obtained by extracting for each individual spectrum used in the averages, the position of the bands and the intensity ratio between D and G modes.

The radial breathing modes (RBM) are related with the contraction and expansion of the tubes, and hence, associated to the diameter and aggregation state. The same frequencies and approximately relative intensity are observed in all RBM modes, indicating same diameter distribution and aggregation state before and after encapsulation following both methods. Similarly, no notable shift of the D and G modes is found between the pristine tubes and the MINTs (Fig S3 b, e and f). The intensity ratio between D and G bands (I_d/I_g) is identical within error between (6,5)-SWCNT (0.035±0.009) and MINT-**1** (self-assembly) (0.038±0.009) and increases slightly for MINT-**1** (preformed metallosquare) (0.087±0.007), as discussed in the main text.

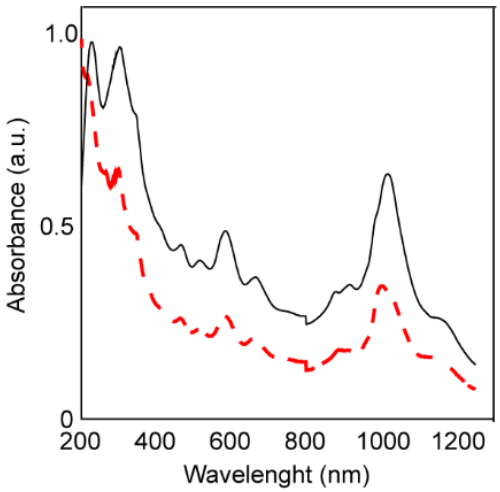

Figure S4. UV/Vis/NIR spectra (D_2O, 1 % sodium dodecyl sulfate (SDS), 298 K) of pristine (6,5)-SWNTs (black) and MINT-**1** (dashed red) prepared using the preformed metallosquare.

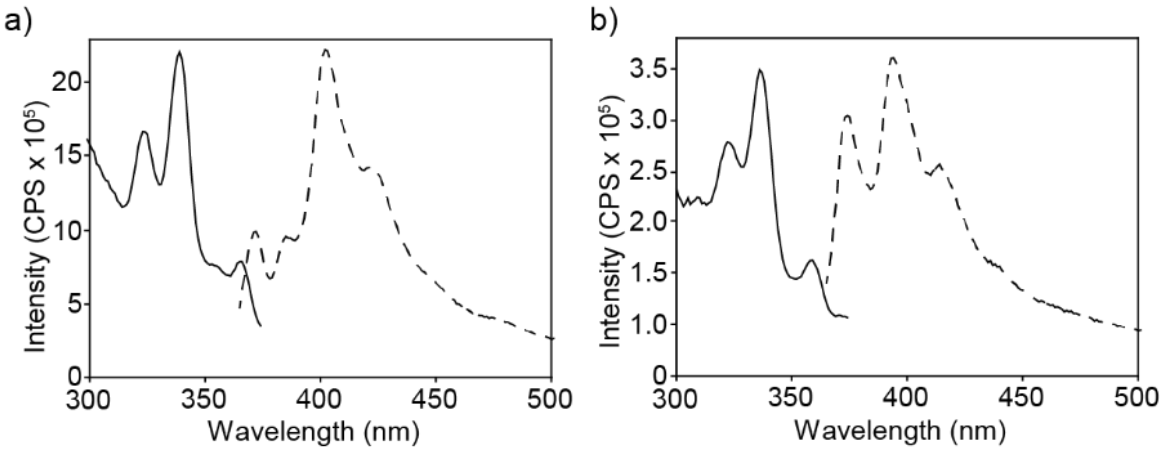

Figure S5. Excitation (black line) and emission (dashed) spectra (D_2O, 1 % sodium dodecyl sulfate (SDS), 298 K) of a) Metallosquare **1** and b) MINT-**1**.

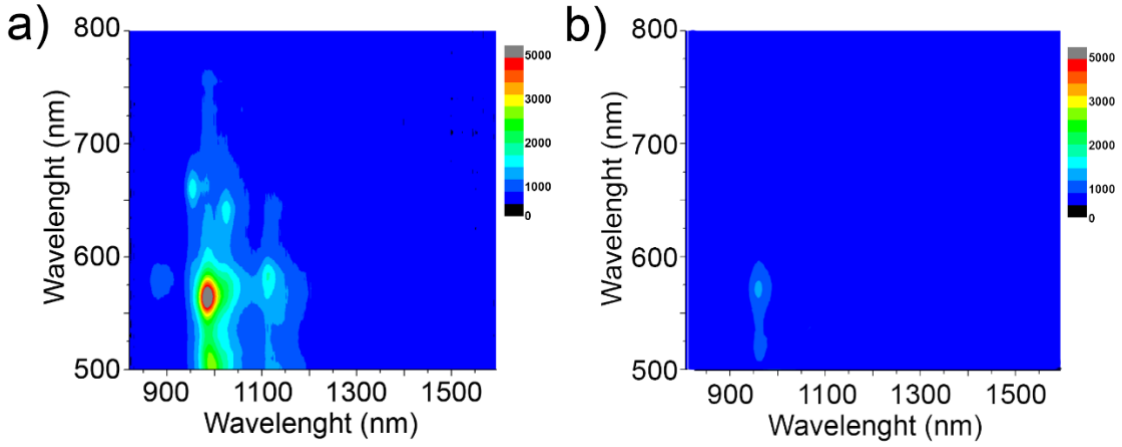

Figure S6. PLE intensity maps (D_2O, 1 % SDS, 298 K) of a) pristine (6,5)-SWNTs and d) MINT-**1** prepared using the preformed metallosquare.

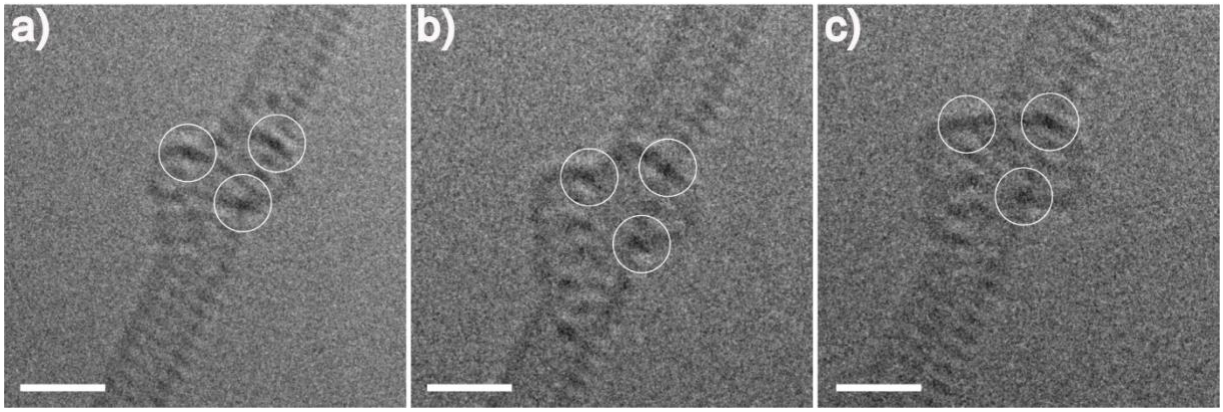

Figure S7. ac-HRTEM micrographs of MINT-**1** showing several Pd atoms. Scale bars are 1 nm.

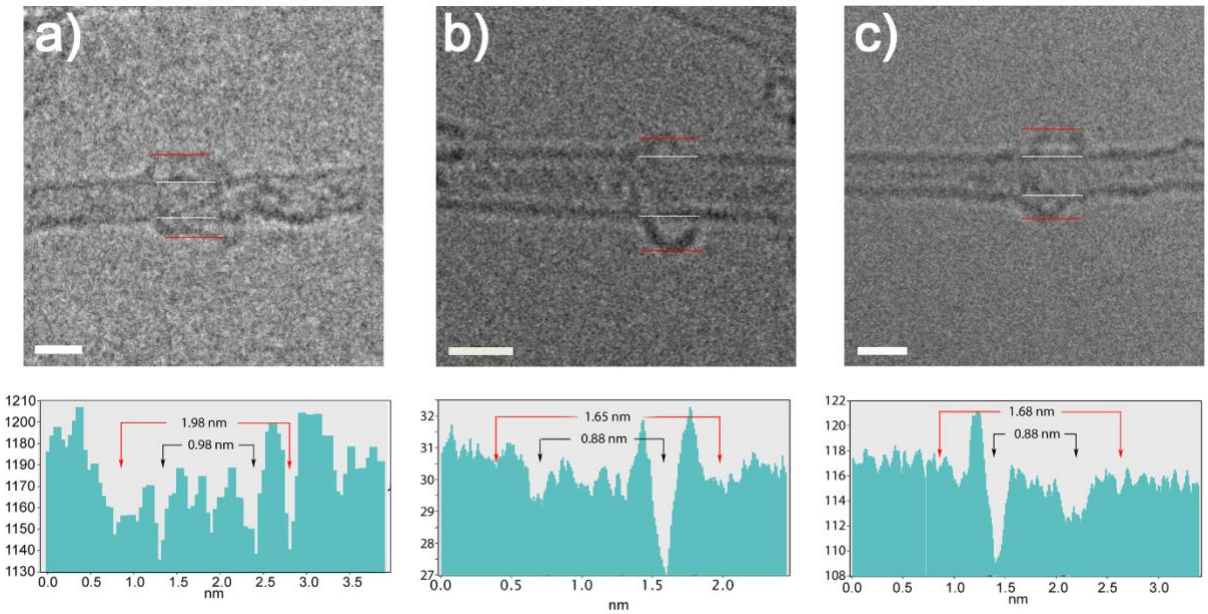

Figure S8. HRTEM micrographs of MINT-**1** showing several SWNT with 1.6-19 nm metallosquares around them. Scale bars are 1 nm.

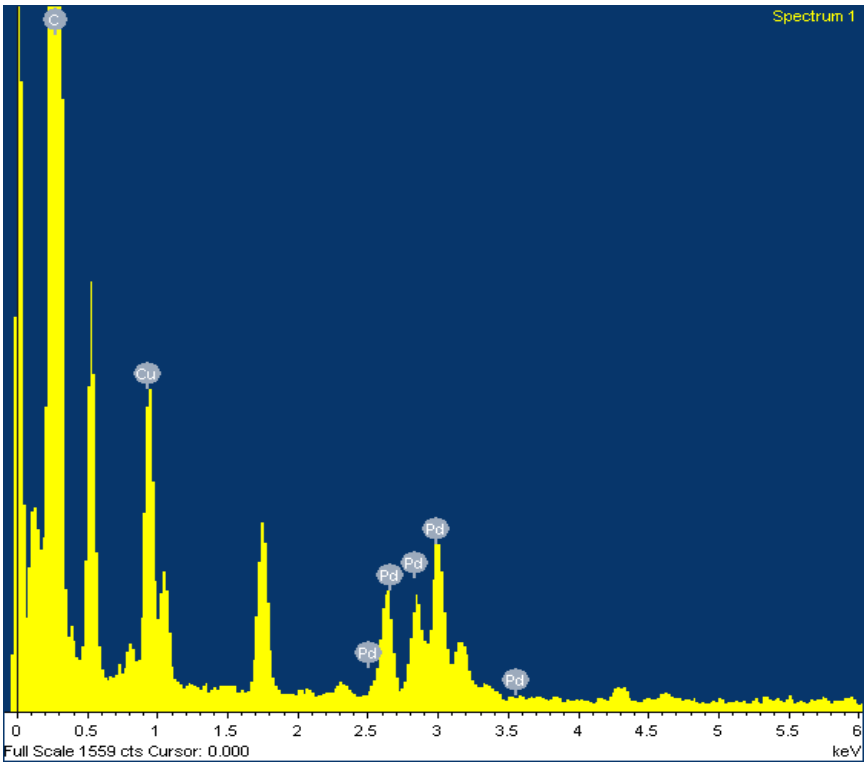

Figure S9. Energy Dispersive X-ray (EDX) spectra of MINT-**1**.

References

[1] V. Martinez-Agramunt, T. Eder, H. Darmandeh, G. Guisado-Barrios, E. Peris, *Angew. Chem. Int. Ed.* **2019**, *58*, 5682-5686.

[2] V. Martinez-Agramunt, S. Ruiz-Botella, E. Peris, *Chem. Eur. J.* **2017**, *23*, 6675-6681.